Available online at www.sciencedirect.com

SCIENCE DIRECT®

Biochimica et Biophysica Acta 1706 (2005) 165–173

BIOCHIMICA ET BIOPHYSICA ACTA

BBA

http://www.elsevier.com/locate/bba

Excited-state dynamics of bacteriorhodopsin probed by broadband femtosecond fluorescence spectroscopy

B. Schmidt, C. Sobotta, B. Heinz, S. Laimgruber, M. Braun, P. Gilch*

Department für Physik, Ludwig-Maximilians-Universität, Oettingenstr. 67, D-80538 München, Germany

Received 18 August 2004; received in revised form 4 October 2004; accepted 20 October 2004
Available online 13 November 2004

Abstract

The impact of varying excitation densities (~0.3 to ~40 photons per molecule) on the ultrafast fluorescence dynamics of bacteriorhodopsin has been studied in a wide spectral range (630–900 nm). For low excitation densities, the fluorescence dynamics can be approximated biexponentially with time constants of <0.15 and ~0.45 ps. The spectrum associated with the fastest time constant peaks at 650 nm, while the 0.45 ps component is most prominent at 750 nm. Superimposed on these kinetics is a shift of the fluorescence maximum with time (dynamic Stokes shift). Higher excitation densities alter the time constants and their amplitudes. These changes are assigned to multi-photon absorptions.

Keywords: Excited state; Bacteriorhodopsin; Femtosecond fluorescence

1. Introduction

Photosynthetic activity in halobacteria is based on the membrane protein bacteriorhodopsin (BR), which acts as a light-driven proton pump [1]. BR consists of 248 amino acids and contains only one chromophore, a retinal molecule, which is linked via a protonated Schiff base to the lysine 216 of the sequence of the protein. In the functionally active light-adapted form of BR, the retinal molecule adopts the all-*trans* configuration. Its function is initiated by the all-*trans*→13-*cis* photoisomerisation of the retinal molecule after photoexcitation. This primary step in the photocycle proceeds on the picosecond time scale and is very efficient (quantum yield ~0.6 [2–5]).

The dynamics of this primary step have been the topic of many time-resolved transient absorption measurements [2,6–12]. Early studies [2,6,7] have revealed a sub-picosecond decay of the first excited state S_1 after optical excitation. Later transient absorption experiments have shown the ultrafast dynamics of BR in more detail. Immediately after excitation, a broad transient hole appears in the absorption spectrum whose amplitude remains constant for about 0.2 ps [9]. For the initial excited state dynamics, a biphasic behaviour with time constants of <0.15 and ~0.45 ps is observed [8,11]. Studies with high time resolution also find an oscillatory behaviour of the transient absorption signal due to wavepacket motion on the excited state and the ground state surface [12–14]. Subsequent to the decay of the S_1 state within ~0.45 ps, a red-shifted absorption band is observed, which can be associated with the buildup of the J intermediate [8,10,11]. This absorption decays within 3–5 ps, indicating the transition of the J intermediate to the K ground state [2,5].

Transient absorption experiments probe processes in the ground state and the excited states. Ground state bleaching, stimulated emission, excited-state absorption, wavepacket motions and absorbance changes due to the formation of photoproducts overlap in the spectra and have to be deconvoluted to distinguish ground state dynamics from excited-state dynamics. This makes it difficult to assign processes to excited states unambiguously. Here, time-

* Corresponding author. Tel.: +49 89 2180 9243; fax: +49 89 2180 9202.
E-mail address: Peter.Gilch@physik.uni-muenchen.de (P. Gilch).

0005-2728/$ - see front matter © 2004 Elsevier B.V. All rights reserved.
doi:10.1016/j.bbabio.2004.10.008

resolved fluorescence spectroscopy is superior since only electronically excited states show fluorescence emission.

So far, only a few time-resolved fluorescence measurements of the primary step of the photocycle of BR in the femtosecond regime have been reported [15,16]. Du and Fleming [15], using the up-conversion method, excited their sample at 608 nm with 3 nJ pulse energy at a repetition rate of 100 kHz. The pump-gate cross-correlation function of these experiments had a FWHM of 0.06–0.07 ps. They reported time constants of 0.09–0.24, 0.6–0.9 and 9.0–13.0 ps. The amplitude of the third time constant has been specified with up to 25%. Haacke et al. [16], also using the up-conversion method, excited their sample at 585 nm with a repetition rate of 80 MHz. A time resolution of 0.25 ps was achieved in these experiments. The data have been treated biexponentially with a short time constant in the sub-picosecond range and a longer time constant of 10 ps. The short time constant varies with the detection wavelength and values increasing from 0.15 to 0.4 ps when moving towards longer wavelengths have been determined. The second time constant of 10 ps carrying only a small amplitude of 4% was found to be wavelength independent. Both experiments draw a similar picture of the fluorescence dynamics of BR; nevertheless, distinct deviations concerning especially the sub-picosecond behaviour and the amplitude of the long time constant are present. These deviations may be due to different excitation conditions and could be clarified by examining the fluorescence dynamics of BR as a function of excitation density.

In this paper, we present results of time-resolved fluorescence measurements with a Kerr gate set-up. The BR sample has been excited from the ground state to the first excited state with different excitation densities ranging from ~0.3 to ~40 photons per molecule. These experiments give new insight in the fluorescence dynamics of BR.

2. Experimental

The femtosecond fluorescence experiments used a set-up based on a Kerr gate described in detail in Ref. [17]. Here only the most important features are described. Briefly, a part of the output (~200 μJ) of a femtosecond laser/amplifier system (Clark CPA 2001 operated at 775 nm with a repetition rate of 1 kHz) pumped a two-stage noncollinear optical parametric amplifier (NOPA) tuned to 565 nm. Compressed NOPA pulses of ~0.05 ps were used as excitation source and were focused onto the sample cell. The excitation pulses were polarised under an angle of 45° with respect to the polarisation plane of the detection. The emission generated by this excitation was collected with reflective optics and imaged onto the Kerr medium (a fused silica plate) placed between two wire grid polarisers.

The excitation density as used in the following is defined as the product of the absorption cross section of BR and the photon density (number of photons per area). It thus represents the number of photons a BR molecule actually 'sees,' when excited with a laser pulse with a certain energy (regardless of the duration of the laser pulse and the concentration of BR molecules). The extinction coefficient of BR of $\sim 6\times10^4$ l mol^{-1} cm^{-1} [2,8] translates into an absorption cross section of $\sim 2.3\times10^{-16}$ cm^2. The photon density is calculated by dividing the number of photons per pulse by the focal area of the excitation spot. The excitation spot diameter was varied between 80 and 160 μm by adjusting an aperture in the beam path and measured by a homebuilt beam profile analyser at the sample location. The energy of the excitation pulses was varied between ~100 and ~3600 nJ per pulse. The excitation densities determined from these parameters range from ~0.3 (pulse energy ~100 nJ at an excitation spot size of 160 μm) to ~40 (pulse energy ~3600 nJ at an excitation spot size of 80 μm) photons per molecule.

An excitation density of 0.3 photons per molecule was shown to be a good compromise between signal to noise ratio and retaining a linear excitation regime. This was verified by performing experiments with an excitation density as low as 0.07 photons per molecule. No systematic deviation between the 0.07 and the 0.3 run could be detected. Trivially, the 0.3 run features a better signal-to-noise ratio and it was thus used to extract the numerical parameters for the linear regime.

Obviously, not only the excitation density but also the light intensity has to be considered when discussing the presence or absence of nonlinear signal contribution. The light intensity of the 0.3 run was equal to ~10^{10} W cm^{-2}, which is of the same size or even lower than the intensities commonly employed in transient absorption experiments on BR [8,10,11,18–20].

The Kerr gate is operated by 0.045 ps NIR laser pulses at 1100 nm generated by a two-stage optical parametric amplifier again pumped by a portion (250 μJ) of the CPA output. The use of NIR pulses at 1100 nm from the OPA instead of fundamental CPA pulses at ~800 nm has the advantage that it opens the spectral region from 700 to 950 nm for fluorescence measurements and improves the temporal resolution. After passing the Kerr gate, the fluorescence light is dispersed by a f=300 mm spectrograph (Acton Research, Spectra Pro 300i) equipped with a 150 lines/mm grating blazed at 800 nm and detected with a liquid nitrogen cooled CCD camera (Princeton Instruments, Spec-10:400B).

The spectra reported here are corrected for the spectral sensitivity of the set-up and for the λ^2-dependence of the gate efficiency (for details, see Ref. [17]). A dielectric mirror placed in front of the spectrometer to reject the light of the gate pulses introduces modulations of the spectra. Though this measurement artefact has been corrected to the best of our knowledge; slight modulations remain nevertheless. These modulations are the origin of the step-like shape of the data in Fig. 2. The duration of the instrumental response function of the set-up is ~0.15 ps (FWHM). Its

width was determined in an independent experiment using spontaneous Raman scattering of water as a reference.

The spectral dependence of time zero induced by the group velocity dispersion of the optical components was derived by the following procedure. The BR sample was replaced by pure water and a white light continuum was generated at an increased pump pulse energy in the water-filled sample cell. The continuum is generated via a nonlinear off-resonant process, which is assumed to be instantaneous on the time scale of our experiment. Therefore, in the sample cell, all spectral components of the continuum are generated at the same instant. Due to dispersion the spectral components then collect wavelength dependent delays on their way to the Kerr medium. These delays were determined by measuring the peak position of the continuum pulse along the time axis at a given wavelength. The resulting time zero dependence is in good agreement with predictions based on the dispersion data of the materials involved. The recorded fluorescence data were corrected using these peak positions. The uncertainty of this time zero correction is estimated to be about ± 0.02 ps and stems mainly from the uncertainty of the exact position of the white light generation in the 1.0-mm-thick sample cell.

For the data presented here at every setting of the delay line the signal was accumulated for 3–6 s or 3000–6000 laser shots, then signal traces of 12–24 scans of the delay line were averaged.

Isolation of bacteriorhodopsin from cells was carried out according to the standard procedure [21]. After lysis of the cells in the presence of DNAse I (Sigma, Steinheim, Germany), the resultant membrane fragments were washed with water and then purified by centrifugation on a sucrose gradient (25–45% w/w). Membrane fractions of buoyant density 1.18 g/ml were collected, washed repeatedly with water and then resuspended in the appropriate buffer solution (pH=7.5) for spectroscopic measurements. The samples were circulated through fused silica flow cells with an optical path length of 1.0 mm.

The absorbance of the sample was 2.0 OD at 568 nm. In the experiments on the intensity effects, this high optical density in combination with the cell length of 1.0 mm can lead to intensity-dependent penetration depths. These in turn might deteriorate the temporal resolution in the high-intensity experiments due to group velocity differences between excitation and fluorescence light. Calculations based on water dispersion data predict maximal apparent shifts in the temporal behaviour of the fluorescence of 0.04 ps. In this prediction, it was assumed that fluorescence light stemming from the whole length of the sample cell contributes to the signal. Yet, the optics used to collect the fluorescence light have a depth of field of 0.5 mm at best. Therefore, these shifts are not expected to be higher than 0.02 ps, being smaller than all other temporal effects discussed here.

Attention was paid to adjust the circulation speed, such that the sample was replaced after each laser shot. BR was light-adapted by continuous illumination with the light of a cold light source (KL 2500 LCD, Schott), which passed OG 550 and KG 5 filters, which suppress the UV and NIR part of the spectrum, respectively.

3. Results

3.1. Low excitation density

In order to investigate BR under conditions similar to native, we performed experiments where the excitation density was kept at 0.3 photons per BR molecule. Under these conditions, nonlinear signal contributions are highly unlikely (see “Experimental” and the next section). BR excited with femtosecond pulses at 565 nm emits a broad and very short lived fluorescence (Fig. 1a). In the spectral range (630 nm–900 nm) covered by the Kerr gate set-up, this emission decays on the sub-picosecond to picosecond time scale. A qualitative analysis shows a predominant fast-decay component in the blue part of the spectra and a somewhat slower (~0.5 ps) decay component in the red part of the spectra. Additionally, there is also a picosecond decay

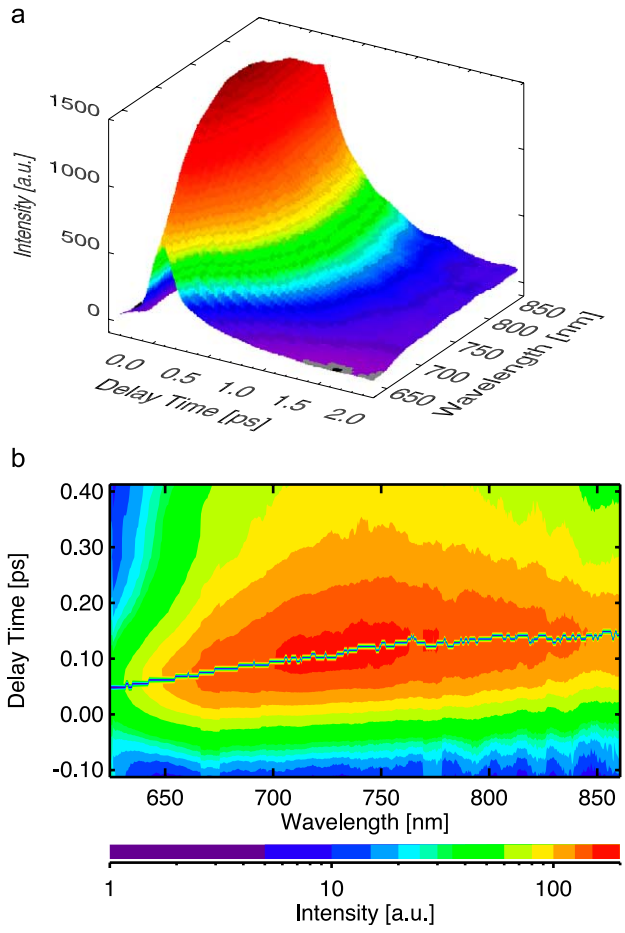

Fig. 1. Time-resolved fluorescence spectra of bacteriorhodopsin excited at low excitation density (~0.3 photons per molecule). (a) Overview. (b) Contour plot of the behaviour around time zero. The line represents the peak of the fluorescence at a given wavelength.

component with a rather small amplitude that can be seen as a small offset at later delay times.

In addition to these decay patterns, a spectral shift on the time scale of a few 0.1 ps is observed. To illustrate this shift, we first adopt the usual representation and plot the fluorescence maxima at a given delay time versus that time (Fig. 2). From this representation, it seems to be clearly evident that the fluorescence emission red shifts with time. Immediately after photoexcitation, the maximum of the fluorescence is located at 650 nm. It then approaches the steady state maximum of 750 nm in about 0.2 ps and remains nearly constant thereafter. Assigning these features to a dynamic Stokes shift seems to be close at hands. However, the wavelength-dependent decay kinetics mentioned above could also mimic such a shift. An analysis of this contribution is easier when using a different representation of the shift dynamics. In Fig. 1b, we mark the peak of the fluorescence intensity along the time axis for a given wavelength. Trivially, in that representation, a shift is also present. The peak moves to longer delay times for increasing wavelengths. This dependence could stem from the aforementioned increasing decay times towards longer wavelengths. For a finite instrumental response time, an increased decay time moves the peak of the fluorescence intensity to later delay times. Simulations demonstrate that this effect is indeed present but not sufficient to explain the experimentally observed shift (see Fig. 3). Depicted is the emission as a function of time (time traces in the following) recorded at the blue (650 nm, crosses) and the red side (800 nm, triangles) of the fluorescence spectrum. The peaks of these time traces are ~0.08 ps apart. We tried to reproduce this effect by fitting the data using a common time zero for the 650 and 800 nm time trace (Fig. 3, solid and dashed line). A prolonged decay time at 800 nm indeed shifts the peak towards longer delay times. However, this accounts for only less than one third of the experimentally observed shift. Thus, we are indeed dealing with a dynamic Stokes shift.

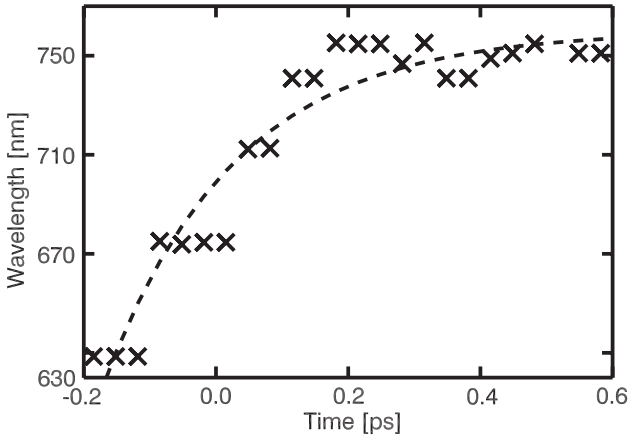

Fig. 2. Dynamic Stokes shift of the fluorescence spectra of bacteriorhodopsin (excitation with low excitation density, ~0.3 photons per molecule). The step-like shape of the data results from the measurement artefact mentioned in "Experimental". The dashed line is inserted as a guide to the eye.

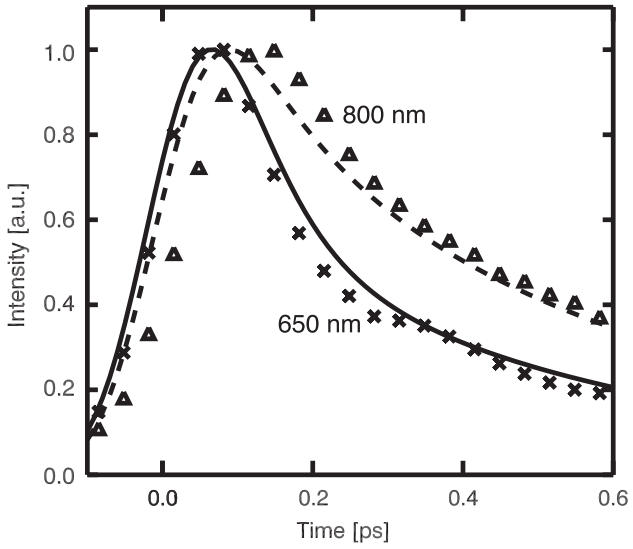

Fig. 3. Normalised time traces of BR. Experimental data points are plotted for 650 nm (crosses) and 800 nm (triangles). Simulated time traces at 650 nm (solid line) and 800 nm (dashed line) are plotted with a common time zero. The simulated shift of the maxima accounts only for one third of the experimentally observed shift.

Dynamic parameters on the fluorescence decay were extracted by a global fitting routine using a multiexponential trial function convoluted with a Gaussian. The Gaussian represents the experimental response function. In this fitting routine, the time zero was treated as a free parameter for all wavelengths to mimic the effects of the dynamic Stokes shift.

The decay traces at all wavelengths >630 nm are nicely reproduced by a trial function using three time constants. The global fit yielded time constants of τ_1~0.05 to 0.15 ps, τ_2~0.45 ps and τ_3~3 to 10 ps. The amplitude related to the fast time constant has its maximum around 650 nm and decays towards the red part of the spectra. The presence of a dynamic Stokes shift indicates that an exponential model cannot handle the data properly in the first few 0.1 ps. Thus, the value for the shortest time constant given above is an approximation—not only numerically but also conceptually. As the second (~0.45 ps) and third (~3 to 10 ps) time constants are longer than the dynamic Stokes shift, a rate model is better justified for the determination of their value. The amplitude maximum of the second time constant peaks around 750 nm, the maximum of the steady state fluorescence (decay associated spectra not shown here). The third time constant has a very broad spectrum with its amplitude maximum shifted even further to longer wavelengths. Since the amplitude is relatively low (<5% of the initial fluorescence emission), only a wide range of 3–10 ps can be given for this time constant.

3.2. High excitation density

In a series of time-resolved fluorescence measurements, the excitation density was raised in several steps from 0.3 to 40 photons per molecule. All experiments with excitation

densities below ~1 photon per molecule yielded results identical to the 0.3 run described above. Experiments with excitation densities ranging from 1 to 40 photons per molecule showed increasing deviations in the spectro-temporal behaviour of the data.

At three different detection wavelengths (650, 730 and 800 nm), decay traces are plotted on a logarithmic scale versus delay time (see Fig. 4). The solid line represents the fluorescence signal of BR at low excitation density of ~0.3 photons per molecule. The dashed line represents the fluorescence signal of BR at high excitation density of ~40 photons per molecule. Two significant changes are observed:

(i) The amplitude of the fastest time constant (<0.15 ps) strongly increases with increasing excitation density. This effect becomes more pronounced at longer wavelengths. Also, a shift of the peak of the fluorescence towards later delay times is observed (see Fig. 4, dashed lines).

(ii) The decay time of the second time constant increases from ~0.45 to ~0.7 ps with increasing excitation density (see also Fig. 4, dashed line). The spectral signature of the amplitudes of the second time constant does not show a dependence on the excitation density.

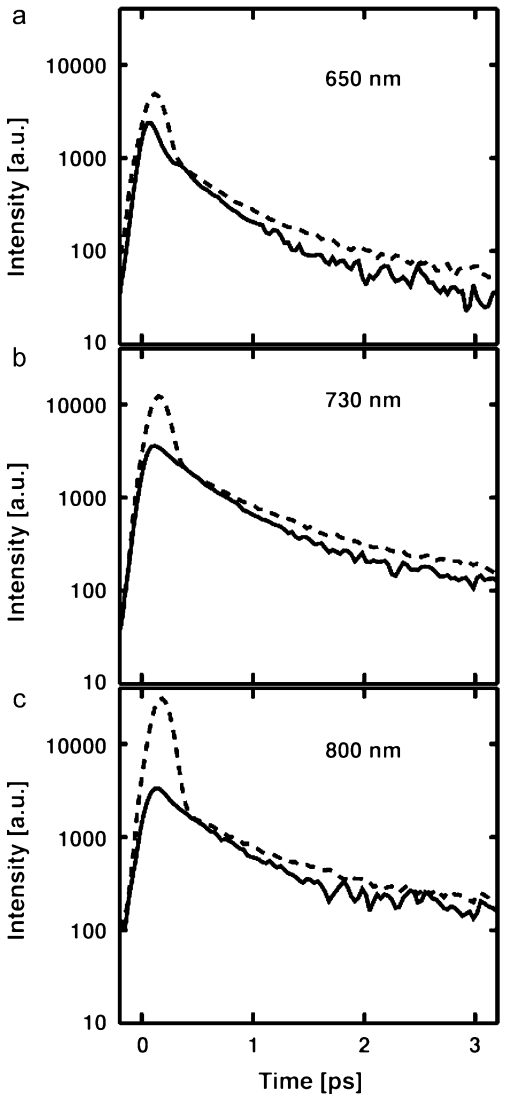

Fig. 4. Time traces at different wavelengths and excitation densities (solid line: ~0.3 photons per molecule, dashed line: ~40 photons per molecule). The different time traces have been normalised with respect to each other at ~0.3 ps. (a) 650 nm; (b) 730 nm; (c) 800 nm.

4. Discussion

The experimental results can be summarised as follows. At low excitation density, a biphasic behaviour with time constants of <0.15 and ~0.45 ps and a dynamic Stokes shift of the fluorescence maxima towards longer wavelengths are observed. At high excitation density, there is at all wavelengths a strong and fast decaying emission. The time constant of the slower component is increased from ~0.45 to ~0.7 ps.

4.1. Low excitation density

Time-resolved fluorescence spectra of molecular systems undergoing ultrafast photoreactions are expected to feature the following characteristics. (i) Due to a (damped) motion on the excited state surface, the energy gap between ground and excited state decreases with time. Such dynamic Stokes shifts are observed in molecular systems with bound and reactive excited state potential energy surfaces. In bound systems, this effect is often due to the dielectric relaxation of the solvent surrounding the excited molecule [22,23]. The shift induced by this relaxation conserves (apart from the ν^3 factor) the spectrally integrated fluorescence intensity. In reactive systems, in addition to these solvent-induced effects, shifts caused by a motion along reactive internal coordinates may take place. (ii) In the course of these large amplitude motions, the Franck–Condon factors for the emission and/or the transition dipole moments may vary causing a variation (usually a reduction) of the spectrally integrated fluorescence intensity [23,24]. Such intensity effects are frequently observed in time-resolved spectra of molecules undergoing ultrafast processes. Examples range from azobenzenes [25,26] over nitroanilines [27] to triarylpyrylium dyes [24]. These experimental findings are in line with quantum chemical calculations [27,28] that often predict a substantial change of the transition dipole moment upon large amplitude motion. (iii) Following these processes in the excited state, its depletion by internal conversion then terminates the fluorescence emission.

In the fluorescence data on BR reported here, all these features can be identified. The peak of the fluorescence spectra moves towards longer wavelengths with a characteristic time of ~0.2 ps (dynamic Stokes shift). Concomitant with that shift, a decay of the overall fluorescence intensity on the very same time scale is observed

(reduction of the emission probability). Finally, with a time constant of 0.45 ps, the greater part of the fluorescence intensity is terminated (internal conversion). The last two features are recovered in transient absorption experiments in which a biphasic decay of excited state signatures with time constants of 0.1–0.2 and ~0.5 ps is observed [8,9,11]. The recovery of the ground state and the formation of photoproducts proceeds with the slower of the two time constants [11]. This further substantiates the notion that the <0.2-ps decay time is *solely* due to processes in the excited state and not to a partial decay of this state.

Surprisingly, the spectral shift reported here has not been mentioned in the literature hitherto. This applies to time-resolved absorption as well as to fluorescence experiments. In fact, most of the transient absorption experiments claim a nearly instantaneous rise of the stimulated emission [10,11,14,18]. There are, however, indications for such a shift. In the data reported by Ye et al. [29], the rise of stimulated emission recorded in the spectral range from 800 to 950 nm is delayed by ~0.02 ps. Evidently, this delay is much smaller than the one described here. Since around the fluorescence maximum, there is nearly no stimulated emission in the transient absorption signal, the existence of an excited state absorbance around the fluorescence maximum was suggested [10,18,19]. As the excited state absorption may respond differently to processes occurring in the excited state than the stimulated emission (or the fluorescence), one could imagine that the spectral dynamics observed in time-resolved absorption and fluorescence experiments need not to be identical. However, in the spectral region of the stimulated emission, no (or only a small tail of this) excited-state absorbance is detected [10,11,18]. Therefore, the origin of the nearly instantaneous rise of the stimulated emission in comparison to the dynamic Stokes shift cannot be explained here on the basis of experimental results and has to remain the object of further investigation.

In the two other femtosecond fluorescence experiments on BR [15,16], no emphasis was laid on the detection of a delayed rise and it cannot be excluded that this effect was therefore missed. Here, to our knowledge, a dynamic Stokes shift is demonstrated for the first time.

In the following, we will compare this Stokes shift with predictions made by the competing models on the primary events in the photocycle of BR. These models (a very recent overview is given in Ref. [30]) can be roughly divided in two groups. The two-state models [8,9,14,30–33] claim that two electronic states—the ground state and one excited state—suffice to describe the photodynamics. In the three-state models [10,34], the potential energy surface of a second excited state comes into play, which is believed to interact with that of the primarily excited state. The first group can be further divided by the fashion in which the motions on the excited state potential surface are treated.

The simplest model is the two-state, one-mode model. Here, the only vibrational mode considered is the torsional mode around the $C_{13}=C_{14}$ double bond, which is either treated inertially or overdamped. In the inertial case [32], the decay of the electronically excited state is fast relative to the vibrational equilibration. In the overdamped case [8,9], the wavepacket generated in the excited state is driven out of the Franck–Condon region in less than 0.2 ps by a reactive potential energy surface along a barrierless path. This movement is accompanied by at least partial vibrational relaxation in the electronically excited state. The conical intersection with the ground state is believed to be situated midway between the all-*trans* and the 13-*cis* geometry. By internal conversion within ~0.5 ps, the molecule relaxes to a hot electronic ground state from where it either relaxes back to the all-*trans* configuration or is fully isomerised into the J intermediate state. In this model, the J intermediate state represents the 13-*cis* electronic ground state from where the molecule relaxes into the K ground state within 3–5 ps.

In the two-mode [14,31,33] model, in addition to the low-frequency torsional coordinate, a high-frequency stretching coordinate is involved. An initial motion out of the Franck–Condon region towards a stationary point along the stretching coordinate results in a relaxation of C–C distances. The wavepacket then moves along the torsional coordinate towards a conical intersection within ~0.5 ps. Also, in this model, the J intermediate is said to have the 13-*cis* configuration.

The many-modes model [30] includes not only a low-frequency torsional but several higher-frequency modes as reaction coordinates. By following a reaction chain during which in each step another vibrational coordinate is excited the isomerised configuration that represents the K ground state is reached within 3.5 ps. The pathways over the C–C stretch and the HOOP (hydrogen out-of-plane) vibrational relaxation lead to the nonreactive, i.e., nonisomerising intermediates I and J in the electronically excited state. The relaxation of these intermediates to the electronic ground state occurs within 0.1–0.2 and 0.5 ps, respectively.

The three-state models [10,34] claim that due to interaction between the S_1 and the S_2 state barriers along the torsional coordinate exist. Following photoexcitation into a relatively flat Franck–Condon active region, this barrier is surmounted in ~0.5 ps. By passing this barrier, the J intermediate is formed, which here is considered to be an excited state species. The decay of the J intermediate partially replenishes the all-*trans* ground state and partially forms the K intermediate.

As the Franck–Condon active region in the three-state model is relatively flat and separated from a steeply sloped reactive region by a small barrier, no Stokes shift is expected to be found. Instead, an instantaneous rise of the fluorescence at all wavelengths is expected. Therefore, the dynamic Stokes shift found here does not fit into this model very well. On the other hand, the two-state overdamped model clearly requires a dynamic Stokes shift on the time scale of the motion of the wavepacket out of the Franck–

Condon active region. The two-states, two-mode model is able to provide an explanation for a dynamic Stokes shift as well. The emission dynamics for early delay times in this model depend on the initial spectral distribution and the time scale of the relaxation along the high frequency coordinate. Another possibility for the appearance of a dynamic Stokes shift could be described by models that include a branching mechanism out of the Franck–Condon active region into distinct molecular pathways. Such an approach would require several reaction coordinates instead of only a torsional one [11]. For example a bifurcation into a reactive and a nonreactive vibrational coordinate could lead to a dynamic Stokes shift on the time scale of the relaxation of the nonreactive vibration while the pathway over the reactive vibrational coordinate would lead to the formation of the isomerised configuration.

Definitely, simple inspection of the experimental data presented here does not allow one to settle the mechanisms of the primary reactions of BR. Such a decision would require an in-depth comparison of simulated data based on the various models with the experimental results. Here, we just note that fluorescence data should simplify this comparison. Contrary to absorption experiments, the excited-state absorptions need not be considered.

Prior to advancing to the high excitation density experiments, the third (picosecond-) time constant has to be discussed. The amplitude related to such a time constant has been found to be very small (<5%) compared to the other two time constants. Since the amplitude is so small, only an estimate of ~3 to 10 ps for this time constant can be given. This is in good agreement with Ref. [16]. The much higher amplitude of up to 25% reported by Ref. [15] might stem from the fact that the sample in this experiment could not be exchanged with each excitation pulse and therefore accumulation of a steady state concentration of intermediates could not be excluded.

Since a fluorescence decay time of $\gtrsim$10 ps is found for BR molecules with a locked retinal chromophore [16,35], that component should not be assigned to the dynamics of the excited state surface of fully functional BR molecules. Instead, we suggest this remaining fluorescence to stem from inactive BR molecules in the sample, like molecules with steric hindrance.

4.2. High excitation density

By applying high-intensity ultrashort laser pulses to the sample, multi-photon and multi-step absorption processes with excitation of higher electronically excited levels can be expected (in the following, we use the term multi-photon absorption for both processes). In fact, indications of such processes in BR have been found by fluorescence [36] and transient absorption experiments [20]. Although the systems are not completely comparable, there is evidence of a saturation behaviour in the reaction centres of Photosystem II of green plants and of the purple bacterium *Rhodobacter sphaeroides* at excitation densities above 0.5 photons per molecule [37]. This is—particularly when considering the slightly different ways of calculating the excitation densities—of the same order as the saturation behaviour found in this work.

The multi-photon process of lowest order to be considered is a 2-photon absorption. For the excitation at 565 nm in the experiments described here excited states in the spectral range of 280 nm are accessible. Since the 2-photon process can occur via a resonant intermediate state ($S_0 \rightarrow S_1 \rightarrow S_n$), it is expected to be rather efficient.

With the occupation of higher excited states S_n of BR, a change in the emission dynamics should occur. One effect of this occupation should be the observation of radiative transitions between the S_n state and other electronic states. Since the S_n state is expected to decay rapidly via internal conversion, the fluorescence emission caused by these radiative transitions should be very short-lived. Nevertheless, such a process should delay the peak of the emission by some time. As the energy gap between higher excited states may be smaller than the $S_1 \rightarrow S_0$ gap, transitions among higher excited states may result in a red-shifted fluorescence emission. Indeed, with increasing excitation density, the ultrafast component (Fig. 4) gains dramatically in amplitude. Apart from the observation of a slight shift of the emission peak towards later delay times, our time resolution does not allow to separate the ultrafast component into a 'normal' low-intensity contribution and a high-intensity part. But the spectral signature of the high-intensity component—it is predominantly observed in the red part of the spectra—underscores the notion that this emission is due to transitions among higher electronic states.

As a second effect of the 2-photon excitation one expects an apparently increased lifetime of the S_1 state. Population transferred from the S_1 to higher excited states has to return to this state prior to its decay. Trivially, the internal conversion from the higher excited states takes time, resulting in the effectively increased lifetime. This increase is experimentally observed. By analysing the second decay component, an increase of the decay time was measured, which ranges in the excitation regime of 1 to 40 photons per molecule between 0.45 and 0.7 ps. Furthermore, the spectrum associated with this decay is not affected by the excitation density. This indicates that under all conditions, the decay of the same state, namely the S_1, is observed. Of course, the transfer to higher excited states might open the route to other reaction channels and/or other regions of the S_1 surface might become accessible. However, such effects if present leave no spectroscopic imprint here.

Both observations can be explained by a 2-photon absorption according to our previous considerations. This leads us to the conclusion that, compared to experiments with low excitation density, the behaviour of BR is changed under high excitation density conditions by preparing BR molecules with a mixture of higher excited states.

5. Conclusion

The photoprocesses of BR have been a topic of research for over 30 years. After absorption of a photon, a reaction cycle with several intermediates (J, K, L, M, N, O) is initiated. Though the time constants associated with the transformation of these intermediates are quite accurately settled, the underlying processes particularly of the primary reaction are still under debate. Since the efficiency of these first steps is the basis for the high overall quantum yield of the BR photocycle, a profound knowledge of these processes is highly desirable. There is consensus that the primary reactions lead to a retinal chromophore isomerised around its $C_{13}=C_{14}$ double bond. The pathways to that isomer—the numbers of vibrational modes and even electronic states involved—are still not resolved in detail. This situation reflects the fact that the problem is very involved theoretically and experimental (mainly spectroscopic) results are often ambiguous. Most experimental information rests on transient absorption spectroscopy. Here, absorption signals of excited states render the comparison with theoretical modelling particularly challenging. Not only the potential energy surface of the state in which the photoreaction takes place has to be calculated but also those of higher electronic states. In fluorescence experiments, the demand on modelling is relaxed; only the ground and one excited state contribute to the signal. Here, for the first time, femtosecond fluorescence experiments on BR employing the Kerr technique have been presented. This technique is particularly suitable to record complete time-dependent fluorescence spectra. By carefully studying the dependence of the fluorescence signals on the excitation densities, some discrepancies found in the literature could be assigned to multi-photon effects. In the one-photon regime, for the first time, a dynamic Stokes shift, i.e., a red shift of fluorescence spectra with time, has been detected. The shift proceeds with a characteristic time of 0.2 ps and is indicative for a fast re-arrangement on the reactive surface. In agreement with other experiments, time constants of <0.15 and ~0.45 ps for the decay of the fluorescence have been determined.

Acknowledgement

We would like to thank Jörg Tittor from the Max Planck Institut für Biochemie at Martinsried for the preparation of the BR samples and Wolfgang Zinth for fruitful discussions and continuous support of this work.

References

[1] U. Haupts, J. Tittor, D. Oesterhelt, Closing in on bacteriorhodopsin: progress in understanding the molecule, Annu. Rev. Biophys. Biomol. Struct. 28 (1999) 367–399.

[2] H.-J. Polland, M. Franz, W. Zinth, W. Kaiser, E. Kölling, D. Oesterhelt, Early picosecond events in the photocycle of bacteriorhodopsin, Biophys. J. 49 (1986) 651–662.

[3] J. Tittor, D. Oesterhelt, The quantum yield of bacteriorhodopsin, FEBS Lett. 263 (1990) 269–273.

[4] M. Rohr, W. Gärtner, G. Schweitzer, A. Holzwarth, S. Braslavsky, Quantum yields of the photochromic equilibrium between bacteriorhodopsin and its bathointermediate K. Femto- and nanosecond optoacoustic spectroscopy, J. Phys. Chem. 96 (1992) 6055–6061.

[5] S. Logunov, M. El-Sayed, L. Song, J. Lanyi, Photoisomerization quantum yield and apparent energy content of the K intermediate in the photocycles of bacteriorhodopsin, its mutants D85N, R82Q, and D212N, and deionized blue bacteriorhodopsin, J. Phys. Chem. 100 (1996) 2391–2398.

[6] M. Nuss, W. Zinth, W. Kaiser, E. Kölling, D. Oesterhelt, Femtosecond spectroscopy of the first events of the photochemical cycle in bacteriorhodopsin, Chem. Phys. Lett. 117 (1985) 1–7.

[7] A. Sharkov, A. Pakulev, Y. Matveetz, Primary events in bacteriorhodopsin probed by subpicosecond spectroscopy, BBA 808 (1985) 94–102.

[8] J. Dobler, W. Zinth, W. Kaiser, D. Oesterhelt, Excited-state reaction dynamics of bacteriorhodopsin studied by femtosecond spectroscopy, Chem. Phys. Lett. 144 (1988) 215–220.

[9] R. Mathies, C. Cruz, W. Pollard, C. Shank, Direct observation of the femtosecond excited-state *cis–trans* isomerisation in bacteriorhodopsin, Science 240 (1988) 777–779.

[10] K. Hasson, F. Gai, P. Anfinrud, The photoisomerization of retinal in bacteriorhodopsin: experimental evidence for a three-state model, Proc. Natl. Acad. Sci. U. S. A. 93 (1996) 15124–15129.

[11] T. Ye, N. Friedman, Y. Gat, G. Atkinson, M. Sheves, M. Ottolenghi, S. Ruhman, On the nature of the primary light-induced events in bacteriorhodopsin: ultrafast spectroscopy of native and $c_{13}=c_{14}$ locked pigments, J. Phys. Chem., B 103 (1999) 5122–5130.

[12] B. Hou, N. Friedman, S. Ruhman, M. Sheves, M. Ottolenghi, Ultrafast spectroscopy of the protonated Schiff bases of free and C13=C14 locked retinals, J. Phys. Chem., B 105 (2001) 7042–7048.

[13] S. Dexheimer, Q. Wang, L. Peteanu, W. Pollard, R. Mathies, C. Shank, Femtosecond impulsive excitation of nonstationary vibrational states in bacteriorhodopsin, Chem. Phys. Lett. 188 (1992) 61–66.

[14] W. Zinth, A. Sieg, P. Huppmann, T. Blankenhorn, D. Oesterhelt, M. Nonella, Femtosecond spectroscopy and model calculations for an understanding of the primary reaction in bacteriorhodopsin, Ultrafast Phenomena XII, Springer Ser. Chem. Phys., vol. 66, 2000, pp. 680–682.

[15] M. Du, G. Fleming, Femtosecond time-resolved fluorescence spectroscopy of bacteriorhodopsin: direct observation of excited state dynamics in the primary step of the proton pump cycle, Biophys. Chemist. 48 (1993) 101–111.

[16] S. Haacke, S. Schenkl, S. Vinzani, M. Chergui, Femtosecond and picosecond fluorescence of native bacteriorhodopsin and a nonisomerizing analog, Biopolymers (Biospectroscopy) 67 (2002) 306–309.

[17] B. Schmidt, S. Laimgruber, W. Zinth, P. Gilch, A broadband Kerr shutter for femtosecond fluorescence spectroscopy, Appl. Phys., B 76 (2003) 809–814.

[18] G. Haran, K. Wynne, A. Xie, Q. He, M. Chance, R.M. Hochstrasser, Excited state dynamics of bacteriorhodopsin revealed by transient stimulated emission spectra, Chem. Phys. Lett. 261 (1996) 389–395.

[19] F. Gai, J. McDonald, P. Anfinrud, Pump-dump-probe spectroscopy of bacteriorhodosin: evidence for a near-IR excited state absorbance, J. Am. Chem. Soc. 119 (1997) 6201–6202.

[20] S.L. Logunov, V.V. Volkov, M. Braun, M.A. El-Sayed, The relaxation dynamics of the excited electronic states of retinal in bacteriorhodopsin by two-pump-probe femtosecond studies, Proc. Natl. Acad. Sci. U. S. A. 98 (2001) 8475–8479.

[21] D. Oesterhelt, W. Stoeckenius, Isolation of the cell membrane of *Halobacterium halobium* and its fractionation into red and purple membrane, Methods Enzymol. 31 (1974) 667–678.

[22] M.L. Horng, J.A. Gardecki, A. Papazyan, M. Maroncelli, Subpicosecond measurements of polar solvation dynamics: coumarin 153 revisited, J. Phys. Chem. 99 (1995) 17311–17337.
[23] M. Glasbeek, H. Zhang, Femtosecond studies of solvation and intramolecular configurational dynamics of fluorophores in liquid solution, Chem. Rev. 104 (2004) 1929–1954.
[24] D. Abramavicius, V. Gulbinas, L. Valkunas, Y.-J. Shiu, K. Liang, M. Hayashi, S. Lin, Molecular twisting and relaxation in the excited state of triarylpyrylium cations, J. Phys. Chem., A 106 (2002) 8864–8869.
[25] Y.-C. Lu, C. Chang, E.W.-G. Diau, Femtosecond fluorescence dynamics of *trans*-azobenzene in hexane on excitation to the $S_1(n,\pi^*)$ state, J. Chin. Chem. Soc. (Taipei) 49 (2002) 693–701.
[26] B. Schmidt, C. Sobotta, S. Malkmus, S. Laimgruber, M. Braun, W. Zinth, P. Gilch, Femtosecond fluorescence and absorption dynamics of an azobenzene with a strong push–pull substitution, J. Phys. Chem., A 108 (2004) 4399–4404.
[27] S. Kovalenko, R. Schanz, V. Farztdinov, H. Hennig, N. Ernsting, Femtosecond relaxation of photoexcited *para*-nitroaniline: solvation, charge transfer, internal conversion and cooling, Chem. Phys. Lett. 323 (2000) 312–322.
[28] D. Markovitsi, H. Sigal, C. Ecoffet, P. Millie, F. Charra, C. Fiorini, J.-M. Nunzi, H. Strzelecka, M. Veber, C. Jallabert, Charge transfer in triaryl pyrylium cations. Theoretical and experimental study, Chem. Phys. 182 (1994) 69–80.
[29] T. Ye, B. Hou, E. Gershgoren, M. Ottolenghi, N. Friedman, M. Sheves, S. Ruhman, Resolving the primary dynamics of bacteriorhodopsin, and Locked analogs in the reactive excited state, Ultrafast Phenomena XII, Springer Ser. Chem. Phys., vol. 66, 2000, pp. 683–685.
[30] H. Abramczyk, Femtosecond primary events in bacteriorhodopsin and its retinal modified analogs: revision of commonly accepted interpretation of electronic spectra of transient intermediates in the bacteriorhodopsin photocycle, J. Chem. Phys. 120 (2004) 11120–11132.
[31] M. Garavelli, F. Negri, M. Olivucci, Initial excited-state relaxation of the isolated 11-*cis* protonated schiff base of retinal: evidence for in-plane motion from ab initio quantum chemical simulation of the resonance Raman spectrum, J. Am. Chem. Soc. 121 (1999) 1023–1029.
[32] R. Birge, Nature of the primary photochemical events in rhodopsin and bacteriorhodopsin, Biochim. Biophys. Acta 1016 (1990) 293–327.
[33] R. Gonzalez-Luque, M. Garavelli, F. Bernardi, M. Merchan, M. Robb, M. Olivucci, Computational evidence in favor of a two-state, two-mode model of the retinal chromophore photoisomerization, Proc. Natl. Acad. Sci. U. S. A. 97 (2000) 9379–9384.
[34] F. Gai, K. Hasson, J. McDonald, P. Anfinrud, Chemical dynamics in proteins: the photoisomerization of retinal in bacteriorhodopsin, Science 279 (1998) 1886–1891.
[35] S. Haacke, S. Vinzani, S. Schenkl, M. Chergui, Spectral and kinetic fluorescence properties of native and nonisomerizing retinal in bacteriorhodopsin, Chem. Phys. Chem. 2 (2001) 310–315.
[36] H. Polland, M. Franz, W. Zinth, W. Kaiser, D. Oesterhelt, Energy transfer from retinal to amino acids—a time-resolved study of the ultraviolet emission of bacteriorhodopsin, Biochim. Biophys. Acta 851 (1986) 407–415.
[37] M.-L. Groot, R. van Grondelle, J.-A. Leegwater, F. van Mourik, Radical pair quantum yield in reaction centers of photosystem II of green plants and of the bacterium *Rhodobacter sphaeroides*. Saturation behavior with sub-picosecond pulses, J. Phys. Chem., B 101 (1997) 7869–7873.